Stokesian dynamics simulations of particle trajectories near a plane

G. Bossis, A. Meunier, and J. D. Sherwood

Citation: Physics of Fluids A: Fluid Dynamics (1989-1993) **3**, 1853 (1991); doi: 10.1063/1.857915
View online: http://dx.doi.org/10.1063/1.857915
View Table of Contents: http://scitation.aip.org/content/aip/journal/pofa/3/8?ver=pdfcov
Published by the AIP Publishing

Stokesian dynamics simulations of particle trajectories near a plane

G. Bossis and A. Meunier
Laboratoire de Physique de la Matière Condensée, Université de Nice, Parc Valrose, 06034 Nice Cedex, France

J. D. Sherwood
Schlumberger Cambridge Research, P.O. Box 153, Cambridge CB3 0HG, England

(Received 10 December 1990; accepted 17 April 1991)

The trajectories of spherical particles close to a plane in shear flow are computed, taking into account lubrication forces and many-body hydrodynamic interactions between spheres, and between spheres and the plane. It is shown that the relative motion of two particles may be reversed by the presence of the plane, and eddylike recirculation motions can occur. The resistance coefficient of a linear chain of N spheres is calculated as a function of the distance of the chain from the plane, and is shown to agree well with a simple model based on a screening coefficient derived from a single pair of spheres.

I. INTRODUCTION

Simulations of concentrated suspensions are usually performed in order to investigate the bulk properties of the suspension, and periodic boundary conditions are frequently adopted in order to reduce as far as possible the effects of the finite size of the simulation. However, in practice, suspensions are bounded, and the presence of boundaries can modify the behavior of the suspension. Wall slip is known to occur when a concentrated suspension flows along a wall (e.g., in pipe flow, or in Couette viscometers),[1] and the resuspension of deposited sediment plays an important role both in slurry transport and in seabed erosion.[2] Other topics of interest include the deposition and adsorption of colloidal particles onto walls in the presence (or absence) of shear flow.[3]

Stokesian dynamics[4] has been successfully used to model unbounded suspensions and to predict such transport properties as the suspension viscosity and particle self-diffusion coefficient.[5-7] Durlofsky and Brady[8] introduced boundary walls into such simulations, dividing each wall into boundary elements, each of which was assumed to be covered by an (unknown) uniform distribution of Stokeslets. However, high accuracy requires a large number of boundary elements, and the size of the computational problem can become excessive.

Here we shall study motion of particles in the presence of a *single* wall. The no-slip condition at the plane wall may be handled by introducing a set of image singularities, and in this way we are able to include the interactions between a sphere and the plane to the same accuracy as the interactions between pairs of spheres. Furthermore, as in previous Stokesian dynamic simulations, we include on a two-body basis lubrication forces both between the spheres themselves, and between the spheres and the plane. The technique is described in Sec. II, and is then used in Sec. III to study the trajectories of two spheres, in shear flow, in the presence of the plane. In Sec. IV we give some results concerning the resistance coefficients of a line of spheres as a function of its distance from the plane.

II. STOKESIAN DYNAMICS IN THE PRESENCE OF A PLANE

The technique of Stokesian dynamics has been described, for an unbounded fluid, in Refs. 4 and 9. We consider an imposed flow with velocity $\mathbf{U}^\infty$ and strain rate E^∞. If the velocities of the particles (including their angular velocities) are represented by $\mathbf{U}$, then, by linearity, the hydrodynamic forces and torques, $\mathbf{F}$, and stresslets S acting on the particles can be expressed as

$$\begin{pmatrix}\mathbf{F}\\ \mathsf{S}\end{pmatrix} = -\mathscr{R}\begin{pmatrix}\mathbf{U}-\mathbf{U}^\infty\\ -\mathsf{E}^\infty\end{pmatrix} = -\begin{pmatrix}\mathsf{R}_{FU} & \mathsf{R}_{FE}\\ \mathsf{R}_{SU} & \mathsf{R}_{SE}\end{pmatrix}\begin{pmatrix}\mathbf{U}-\mathbf{U}^\infty\\ -\mathsf{E}^\infty\end{pmatrix}, \tag{1}$$

where for N particles the force $\mathbf{F}$ and velocity $\mathbf{U}$ have $6N$ components ($3N$ for translation, $3N$ for rotation). The symmetric, traceless parts of

$$\mathsf{S} = (S_{11}, S_{12}, S_{13}, S_{23}, S_{22})$$

and

$$\mathsf{E}^\infty = (E^\infty_{11} - E^\infty_{33}, 2E^\infty_{12}, 2E^\infty_{13}, 2E^\infty_{23}, E^\infty_{22} - E^\infty_{33})$$

each have $5N$ components. The suspending fluid is assumed Newtonian, with viscosity μ, and the particles are spheres of radius a. We scale all forces by $6\pi\mu a$, torques by $6\pi\mu a^2$, and stresslets by $\frac{20}{3}\pi\mu a^3$. The inverse relation to (1) is

$$\begin{pmatrix}\mathbf{U}-\mathbf{U}^\infty\\ -\mathsf{E}^\infty\end{pmatrix} = \mathscr{M}\begin{pmatrix}\mathbf{F}\\ \mathsf{S}\end{pmatrix} = \begin{pmatrix}\mathsf{M}_{UF} & \mathsf{M}_{US}\\ \mathsf{M}_{ES} & \mathsf{M}_{ES}\end{pmatrix}\begin{pmatrix}\mathbf{F}\\ \mathsf{S}\end{pmatrix}.$$

Durlofsky *et al.*[9] explain how an approximation to $\mathscr{R}$ that includes many-body interactions may be obtained: far-field two-body interactions between pairs of spheres give an approximation $\mathscr{M}^\infty$, which is then inverted to produce $\mathscr{R} \simeq (M^\infty)^{-1}$. Lubrication forces may be introduced by adding to $(M^\infty)^{-1}$ the pairwise two-body interactions $\mathscr{R}_{2b}$, and then, to preclude double counting of long-range interactions, subtracting the far-field two-body interactions $\mathscr{R}^\infty_{2b}$. Hence

$$\mathscr{R} \simeq (M^\infty)^{-1} + \mathscr{R}_{2b} - \mathscr{R}^\infty_{2b}. \tag{2}$$

 0899-8213/91/081853-06$02.00

Once we have obtained $\mathscr{R}$, we may invert (1) to obtain the velocities of the spheres relative to the imposed flow

$$\mathbf{U} - \mathbf{U}^\infty = \mathsf{R}_{FU}^{-1}(\mathbf{F} + \mathsf{R}_{FE}:\mathsf{E}^\infty). \tag{3}$$

The presence of the plane modifies not only the two-body interactions between pairs of spheres, but also the motion of a single sphere (the self-interaction term). For example, the force $\mathbf{F}^\alpha$ on a particle α with velocity $\mathbf{U}^\alpha$ will be given by

$$\mathbf{F}^\alpha = \left(\mathsf{I} + (\mathsf{R}_\alpha^{\mathrm{SP}})_{FU} + \sum_{\beta\neq\alpha}(\mathsf{R}_{\alpha\beta}^{\mathrm{SS}})_{FU}\right)\cdot(\mathbf{U}^\alpha - \mathbf{U}^\infty),$$

where $\mathsf{R}_{\alpha\beta}^{\mathrm{SS}}$ includes the modified sphere–sphere interactions, and $\mathsf{I} + (\mathsf{R}_\alpha^{\mathrm{SP}})_{FU}$ is the resistance coefficient for the single sphere α in the presence of the plane. Similarly, the force on an isolated sphere due to the imposed straining motion E^∞ is modified to become

$$\mathbf{F}^\alpha = \left((\mathsf{R}_\alpha^{\mathrm{SP}})_{FE} + \sum_{\beta\neq\alpha}(\mathsf{R}_{\alpha\beta}^{\mathrm{SS}})_{FE}\right)\cdot(\mathsf{E}^\infty).$$

The hydrodynamic interaction between a single sphere and a plane has been considered by many authors, and is a special case of the interaction between two spheres, one of which has infinite radius. Details are relegated to the Appendix. Each of the submatrices $\mathsf{R}_{FU}^{\mathrm{SP}}$, $\mathsf{R}_{FU}^{\mathrm{SS}}$, $\mathsf{R}_{FE}^{\mathrm{SP}}$, $\mathsf{R}_{FE}^{\mathrm{SS}}$, includes the lubrication terms calculated either between two spheres or between a sphere and the plane. The total matrix including the interaction with the plane is formed in the same way as in Eq. (2). No analytic results are available for the motion of two spheres in the presence of a plane, and we next consider the far-field interactions between two such spheres.

Consider (Fig. 1) a point force $\mathbf{f}$ located a distance h above the plane. The velocity field at $\mathbf{x}$ generated by a point force at $\mathbf{y}$ has the form[10]

$$\begin{aligned} v_i(\mathbf{x},\mathbf{y}) &= G_{ij}(\mathbf{x},\mathbf{y})f_j(\mathbf{y}) \\ &= [J_{ij}(\mathbf{x},\mathbf{y}) + G_{ij}^{im}(\mathbf{x},\mathbf{y}')]f_j(\mathbf{y}). \end{aligned}$$

Here, J is the Stokes propagator corresponding to a point force in an unbounded medium, and depends only on $\mathbf{r} = \mathbf{x} - \mathbf{y}$:

$$J_{ij}(\mathbf{x},\mathbf{y}) = \frac{1}{8\pi\mu a}\left(\frac{\delta_{ij}}{r} + \frac{r_i r_j}{r^3}\right).$$

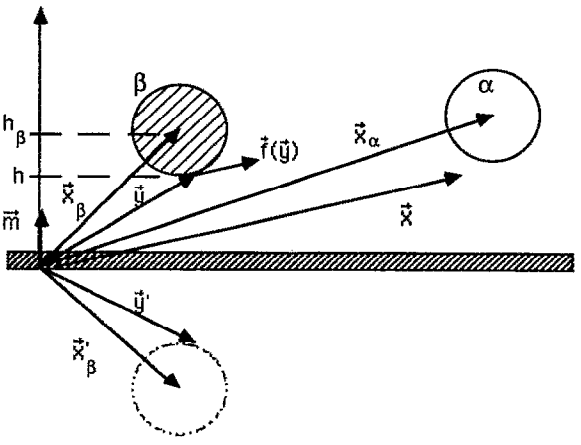

FIG. 1. Diagram showing the notation used when calculating the hydrodynamic interactions between two spheres α and β in the presence of a plane.

Here, $\mathsf{G}^{im}\cdot\mathbf{f}$ is the velocity field due to the image system at the mirror position $\mathbf{y}' = \mathbf{y} - 2hm$, where m is the unit normal to the plane, and G^{im} was given by Blake:[10]

$$\begin{aligned} G_{ij}^{im}(\mathbf{x},\mathbf{y}') = &-J_{ij}(\mathbf{x},\mathbf{y}') \\ &+ h^2(\delta_{jm} - 2\delta_{j3}\delta_{m3})\nabla_{y'}^2 J_{im}(\mathbf{x},\mathbf{y}') \\ &+ 2h\delta_{q3}(\delta_{jm} - 2\delta_{j3}\delta_{m3})\frac{\partial}{\partial y'_m}J_{iq}(\mathbf{x},\mathbf{y}'), \end{aligned}$$

where δ_{ij} is the Kronecker symbol. Here G^{im} ensures that the velocity field is zero on the plane. If we now consider that $F_j(\mathbf{y})$ is the force density on the surface S of sphere β (center $\mathbf{x}_\beta$), we can expand $\mathsf{G}(\mathbf{x},\mathbf{y})$ about $\mathsf{G}(\mathbf{x},\mathbf{x}_\beta)$ to obtain

$$\begin{aligned} v_i(\mathbf{x}) &= \int_S G_{ij}(\mathbf{x},\mathbf{y})F_j(\mathbf{y})dS_y \\ &= \left[\left(1 + \frac{a^2}{6}\nabla_y^2\right)G_{ij}(\mathbf{x},\mathbf{y})\right]_{y=x_\beta} F_j^\beta \\ &\quad + \left[\left(1 + \frac{a^2}{10}\nabla_y^2\right)\frac{\partial}{\partial y_k}G_{ij}(\mathbf{x},\mathbf{y})\right]_{y=x_\beta} S_{kj}^\beta \\ &\quad + \left(\frac{\partial}{\partial y_k}G_{ij}(\mathbf{x},\mathbf{y})\right)_{y=x_\beta} L_{kj}^\beta. \end{aligned} \tag{4}$$

Here, $\mathbf{F}^\beta = \int_S \mathbf{F}\,dS_y$ is the total force excerted on the fluid by the sphere β and S^β and L^β are, respectively, the symmetric traceless, and antisymmetric parts of the dipole term $\int_S(\mathbf{y} - \mathbf{x}_\beta)\mathbf{F}\,dS_y$. The terms in $a^2\nabla_y^2$ have been included in (4), as these give exact results for an isolated sphere in unbounded fluid subjected to a force $\mathbf{F}$ or subjected to a straining motion. However, other higher-order terms have been neglected, as discussed in Ref. 9. Once we have obtained the velocity field $\mathbf{v}(\mathbf{x})$, we can compute the velocity $\mathbf{U}^\alpha$, angular velocity $\boldsymbol{\Omega}^\alpha$ and stresslet S^α of a sphere at $\mathbf{x}_\alpha$ by means of Faxen's relations (see, e.g., Ref. 11)

$$U_i^\alpha = F_i^\alpha/6\pi\mu a + [1 + (a^2/6)\nabla^2]v_i(\mathbf{x}_\alpha), \tag{5}$$

$$\Omega_i^\alpha = L_i^\alpha/8\pi\mu a^2 + \tfrac{1}{2}\epsilon_{ijk}\partial_j v_k(\mathbf{x}_\alpha), \tag{6}$$

$$\begin{aligned} 0 = (3/20\pi\mu a^3)\mathsf{S}_{ij}^\alpha &+ [1 + (a^2/10)\nabla^2][\partial_i v_j(\mathbf{x}_\alpha) \\ &+ \partial_j v_i(\mathbf{x}_\alpha)], \end{aligned} \tag{7}$$

where $\partial_i = \partial/\partial x_i$ and $\mathbf{F}_i^\alpha$, $\mathbf{L}_i^\alpha$ are, respectively, the force and couple on sphere α. Combining Eqs. (4) and (5)–(7), we obtain a set of relations between the velocity of sphere α and the two first moments of the force density on sphere β, and thus, as in Ref. 9, we can obtain the far-field approximation to the mobility matrix (2). For example, the submatrix M_{UF} will have the form

$$\begin{aligned} (M_{UF}^{\alpha\beta})_{ij} &= [1 + (a^2/6)\nabla_{x_\alpha}^2][1 + (a^2/6)\nabla_{x_\beta}^2] \\ &\quad \times [J_{ij}(\mathbf{x}_\alpha,\mathbf{x}_\beta) + G_{ij}^{im}(\mathbf{x}_\alpha,\mathbf{x}'_\beta)], \\ (M_{UF}^{\alpha\alpha})_{ij} &= 1 + [1 + (a^2/6)\nabla_{x_\alpha}^2] \\ &\quad \times [1 + (a^2/6)\nabla_{x'_\alpha}^2]G_{ij}^{im}(\mathbf{x}_\alpha,\mathbf{x}'_\alpha), \end{aligned}$$

and other terms are given by Meunier.[12] Thus we have obtained the total mobility matrix $\mathscr{M}^\infty$ (of dimension $11N \times 11N$), based on the first two multipoles of the force densities over the spheres in the presence of the plane. Inverting this matrix gives the many-body interactions be-

tween the N spheres and the plane. The number of unknowns remains proportional to the number of spheres, with no additional unknown force densities introduced to account for the elements of the plane. The price to be paid is a more complicated form for the elements of the mobility matrix, but these do not have to be computed at every time step,[9] so the computational time is not greatly increased.

III. THE TRAJECTORIES OF TWO SPHERES

We now consider the motion of two identical spheres above a plane $z=0$ when a shear flow $(u_x,u_y,u_z)=(\dot{\gamma}z,0,0)$ is imposed. We scale all lengths by the sphere radius a, velocities by $\dot{\gamma}a$, and assume that the spheres start (and remain) in the plane $y=0$. If the spheres are force-free, then by (3) their velocities are

$$\mathbf{U}=\mathbf{U}^{\infty}+\mathsf{R}_{FU}^{-1}\cdot\mathsf{R}_{FE}\cdot\mathsf{E}^{\infty}.$$

Some typical results are given in Fig. 2. We consider two spheres, one of which (the reference particle) is initially at a height $z_0=2$ above the plane. The second, test sphere is initially at (x_1,z_1), and we suppose $x_1-x_0=-3$ at $t=0$. Figure 2 shows the trajectory of the test sphere, using x_1-x_0 (relative coordinates) for the x direction, and z_1 (the absolute position of the test sphere above the plane) for the z coordinate.

We consider first the case with initial condition $z_1=z_0+\Delta z=2.2$ at $t=0$. Curve 1 is the trajectory of the test particle in the *absence* of the plane. As expected, the test particle moves up and over the reference particle. Curve 2 shows the trajectory in the presence of the plane, starting from initial conditions identical to curve 1. We see that the test particle moves *downward*, rather than upward, and that it is left behind by the reference particle. Eventually, when the horizontal separation x_0-x_1 has increased to 7, the relative horizontal velocity $v_x^1-v_x^0$ reverses in direction.

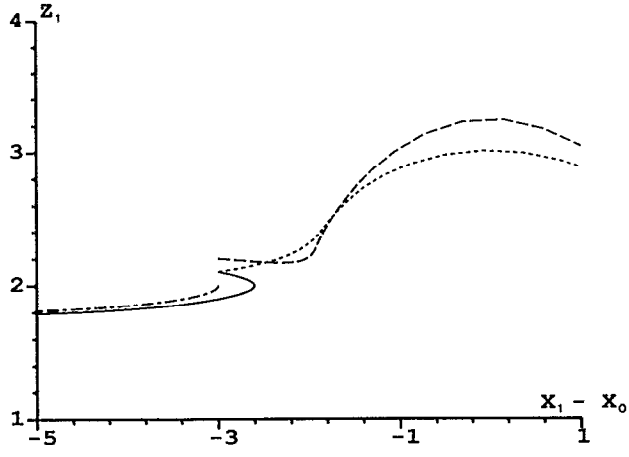

FIG. 2. Trajectories of sphere 1, in the presence of a second sphere initially at $x_0=0$, $z_0=2$, either with or without a plane at $z=0$. The trajectories show the absolute height z_1 of sphere 1 above the plane, and the horizontal position x_1-x_0 relative to sphere 0. Trajectory 1 (- - - -), no plane, initial position $x_1=-3$, $z_1=2.2$; trajectory 2 (—), plane at $z=0$, initial position $x_1=-3$, $z_1=2.2$; trajectory 3 (- - -), plane at $z=0$, initial position $x_1=-3$, $z_1=2.1$; trajectory 4 (— —), plane at $z=0$, initial position $x_1=-3$, $z_1=2.3$.

Similar behavior is shown by a sphere starting at $\Delta z=0.1$ (curve 3). However, if the initial vertical separation is increased to $\Delta z=0.3$ (curve 4), the particles rotate over each other (as in unbounded shear flow) rather than separate (as on curves 2 and 3).

The relative motion of the particles is very sensitive to their positions relative to each other and to the plane. This can be seen for two spheres placed at the same height $z_1=z_0$ above the plane, with the sphere $n°1$ placed upstream. In Fig. 3 we show the vertical velocity v_z^1 of sphere $n°1$ (which is opposite to v_z^0, the vertical velocity of sphere $n°0$) as a function of the separation $\epsilon=x_0-x_1-2$ between the surfaces of the spheres. The curves 1, 2, 3, and 4 correspond to $z_1=1.01$, 1.1, 2.0, and 4.0, respectively. When $z_1=1.01$ (curve 1) the relative velocity becomes negative at a horizontal separation $\epsilon=0.1$, but, because of lubrication forces between the plane and the spheres, the vertical velocities are never large in this case. The maximum negative velocity occurs when the spheres are at a height $z_1\simeq 2$ above the plane, with $\epsilon=1$ ($x_0-x_1=3$). As z_1 increases to values greater than 2, so the influence of the wall diminishes and the negative velocities are reduced. At sufficiently large horizontal separations the relative vertical velocity changes sign and becomes positive, before tending ultimately to zero. This second reversal of sign occurs when $x_1-x_0=8.7$ in the case $z_1=2$ (curve 3).

When the two spheres are very close together we expect them to rotate as a doublet, while at very large separations we can predict their relative motion from the image system derived by Blake. Thus only the region of reversed velocities remains to be explained. To this end we can examine the flow generated by a stresslet in the presence (or absence) of a plane. The stresslet acting on the fluid is equal and opposite to that exerted on the particle by the flow. In the absence of the plane it produces a flow with velocity $v_z>0$ on the upstream side $x<0$, and $v_z<0$ on the downstream side [Fig. 4(a)]. In the presence of a plane [Fig. 4(b)] fluid cannot be drawn from the half-space below the particle, and must come from above, creating an eddy on the upstream side $x<0$. A second particle placed in this eddy will be pushed

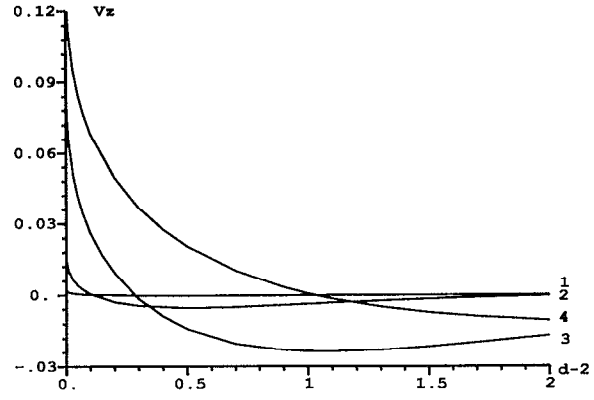

FIG. 3. Two spheres are placed in a shear flow at the same height z_0 above the plane $z=0$. The figure shows the upward vertical velocity v_z of the upstream particle as a function of the separation $\epsilon=x_1-x_0-2$ between the spheres: (1) $z_0=1.01$; (2) $z_0=1.1$; (3) $z_0=2.0$; (4) $z_0=4.0$.

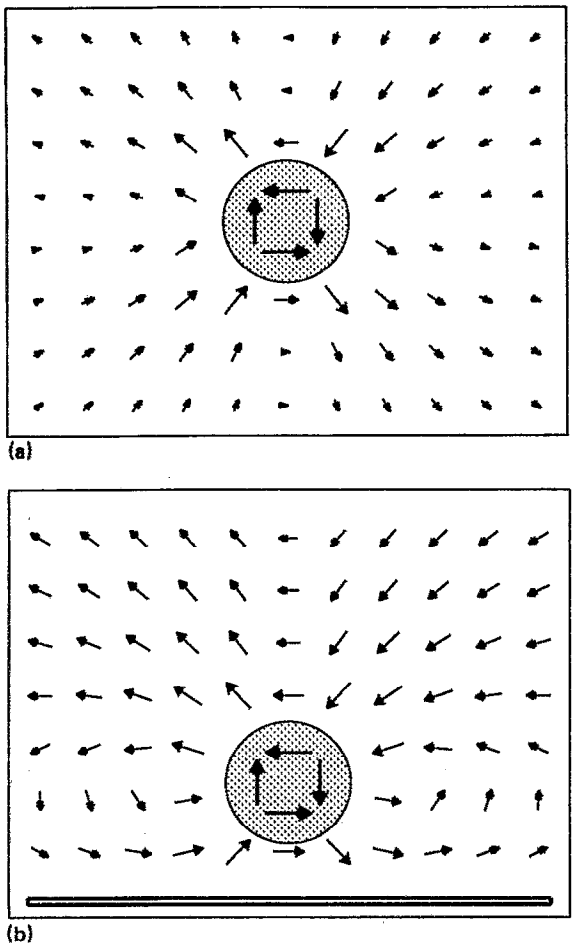

FIG. 4. Modification of the flow pattern due to a stresslet by the presence of a plane: (a) without plane, flow induced by the stresslet in an infinite fluid; (b) with a plane. The plane forces fluid to come from above the particle, rather than from below. This velocity field can pull upstream particles toward the plane, leading subsequently to separation of the particles.

toward the plane and this explains the negative part of velocities in Fig. 3. A similar eddy is created on the downstream side. Some more insight may be gained from the simpler example of a cylinder. If the cylinder is in an unbounded shear flow, then, as shown in Ref. 13 there are regions of backflow and reversed vertical velocities if the cylinder is impeded from rotating freely. When the cylinder is freely suspended above a plane (again in shear flow), the dominant effect of the plane is to impede the rotation (and translation) of the cylinder. Regions of backflow occur, and the second reversal of vertical velocities at large distances from the cylinder leads to closed eddies rather than streamlines which go off to infinity. This explains the motion of the spheres in Fig. 2, though in this case the presence of a second sphere will affect the motion of the first particle, leading, in the presence of the wall, to a complicated three-body problem.

IV. THE RESISTANCE COEFFICIENTS OF A CHAIN OF SPHERES

The velocity $\mathbf{U}$ of a particle is related to the applied force $\mathbf{F} = \boldsymbol{\xi}\cdot\mathbf{U}$ by means of the resistance tensor $\boldsymbol{\xi}$, which frequently simplifies to some simple friction coefficients ξ_i when use is made of any symmetries possesed by the particle. We scale all forces by $6\pi a\mu U$ and all lengths by the sphere radius a. It is known from slender-body theory[14] that the friction coefficient of an elongated body of aspect ratio L (such as a line of N spheres of dimensional half-length $L^* = Na$ and radius a), oriented along the x axis, scales (in the limit $L \to \infty$) as

$$\xi_x^{SB} \sim \tfrac{2}{3}L\,(\ln 2L - \tfrac{1}{2})^{-1}, \tag{8}$$

$$\xi_y^{SB} = \xi_z^{SB} \sim \tfrac{4}{3}L\,(\ln 2L + \tfrac{1}{2})^{-1}. \tag{9}$$

where the above results are in general only accurate to leading order in $(\ln L)^{-1}$ (Ref. 14). In Ref. 9 a comparison against the predictions of slender-body theory was found to be a useful test of the results of Stokesian dynamics, and we repeat here similar tests in the presence of a wall. Our interest lies in the possibility of applying these results to the motion of chains of colloidal spheres. Such chains can be formed from a suspension of individual particles by the application of an electric field, and, when observed under a microscope, their motion is affected by the presence of the microscope slide.

The friction coefficients may be obtained by taking the sum of the forces on each sphere in the chain. In terms of the resistance matrix, this is

$$\xi_i = \sum_{\alpha=\beta=1}^{N} R_{ii}^{\alpha\beta}, \quad i = x,y,z.$$

We consider a line of five spheres parallel to the plane, at a center-to-center separation $r - 2 = 10^{-5}$. In Fig. 5 we plot ξ_x (for motion parallel to the chain of spheres), ξ_y (perpendicular to the chain, but still parallel to the plane), and ξ_z (perpendicular to the plane) as a function of the height h of the chain above the plane.

At great distances from the plane, the friction coefficients ξ_y and ξ_z should become equal. This is approximately true by $h = 50$, though the chain of particles is too short for the asymptotic results (8) and (9) to hold, as is well known

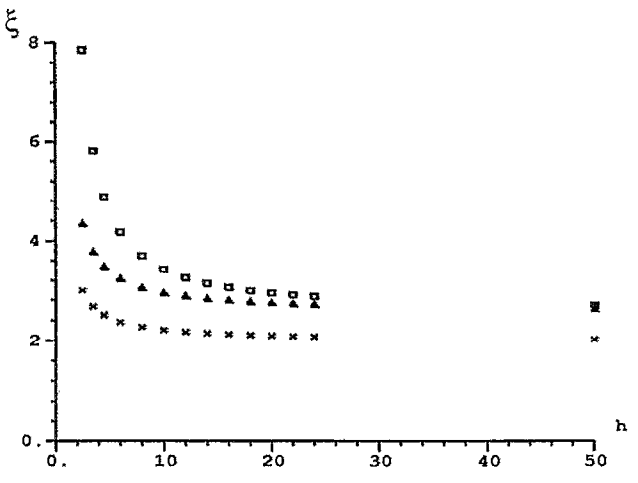

FIG. 5. Friction coefficients for a chain of five spheres aligned with major axis in the x direction parallel to the plane $z = 0$, as a function of the height h above the plane. $\times$: ξ_x; $\triangle$: ξ_y; $\square$: ξ_z.

TABLE I. Values of the friction coefficient, ξ_x, parallel to the axis of the chain for different numbers, N, of spheres inside the chain and different heights, h, of the chain above the plane. SD is the numerical result obtained by Stokesian dynamics incorparating the plane. $C_s = 2\xi_x^{(1)} - \xi_x^{(2)}$ is almost constant (≈ 1.20) for heights h less than 10^{-2}.

h	$1+10^{-6}$		$1+10^{-2}$		2		50		
ξ_x	SD	Eq. (10)	SD	Eq. (10)	SD	Eq. (10)	SD	Eq. (10)	Eq. (8)
$N=1$	8.3	⋯	3.4	⋯	1.4	⋯	1.0	⋯	⋯
2	15.4	⋯	5.6	⋯	1.9	⋯	1.3	⋯	⋯
5	36.6	36.8	12.2	12.3	3.3	3.5	2.0	2.2	1.85
10	71.9	72.3	23.0	23.3	5.6	6.1	3.0	3.7	2.67
20	142.5	143.5	44.8	45.4	10.2	11.3	4.9	6.7	4.18
C_s	1.215		1.197		0.858		0.7136		

from previous studies.[14,15] The drag is increased by the presence of the wall, and a far-field approximation,[16] valid when $h \gg L$ gives

$$\xi_x = \frac{2}{3}\frac{L}{(\ln 2L - \frac{1}{2})}\left(1 + \frac{3}{8}\frac{L/h}{(\ln 2L - \frac{1}{2})}\right),$$

$$\xi_y = \frac{4}{3}\frac{L}{(\ln 2L + \frac{1}{2})}\left(1 + \frac{3}{4}\frac{L/h}{(\ln 2L + \frac{1}{2})}\right),$$

$$\xi_z = \frac{4}{3}\frac{L}{(\ln 2L + \frac{1}{2})}\left(1 + \frac{3}{2}\frac{L/h}{(\ln 2L + \frac{1}{2})}\right).$$

De Mestre and Russel[17,18] replaced the point image system by a line distribution of images, and obtained friction coefficients valid for $h \gg 1$. Russel *et al.*[15] concluded that for the cases they studied the major source of error was the basic inadequacy of the slender-body predictions for all but the highest of aspect ratios, and turned directly to a numerical approach.

For a separation $h \ll L$ we can turn to analytic results for infinite cylinders adjacent to a plane. Results for ξ_y and ξ_z are given in Ref. 19, while standard solutions for the Laplace equation in bipolar coordinates give $\xi_x = 4\pi\mu L/\cosh^{-1} h$.

When h is similar to the radius of the spheres, it is no longer appropriate to approximate the line of particles by a uniform cylinder. However, when the separation $\epsilon = h - 1$ between the spheres and the plane is small ($\epsilon \ll 10^{-2}$), we can make analytic predictions on the basis of the lubrication forces between individual spheres and the plane. Thus the friction coefficient for tangential motion of a single sphere close to a plane is

$$\xi_x^{(1)} = -\tfrac{8}{15}\ln\epsilon + 0.9588.$$

The friction coefficient $\xi_x^{(2)}$ for two spheres (almost in contact) will be less than twice that of a single sphere, because of screening. If we set

$$C_s = 2\xi_x^{(1)} - \xi^{(2)},$$

we see (Table I) that C_s tends to a constant (1.206 ± 0.01) as $\epsilon \to 0$. Here, C_s decreases to 0.7 when h becomes large. Assuming now that this screening effect is pairwise additive, we would expect the friction coefficient for a chain of N spheres to increase as

$$\xi_x^{(N)} = N\xi_x^{(1)} - (N-1)C_s$$
$$= \xi^{(1)} + (N-1)(\xi^{(2)} - \xi^{(1)}). \quad (10)$$

Inserting the value $C_s = 1.206$ into (10) gives

$$\xi_x^{(N)} = N(-\tfrac{8}{15}\ln\epsilon - 0.247) + 1.206. \quad (11)$$

We see from Table I that (11) gives good predictions for $\epsilon \ll 10^{-2}$. Once ϵ becomes larger, the friction coefficient, as predicted by slender-body analysis, varies as $N/\ln N$ and the predictions of (11), linear in N, grow too rapidly as N increases. Similar asymptotic results for the limit $\epsilon \to 0$ can be obtained for ξ_y, while ξ_z diverges as ϵ^{-1} in the limit $\epsilon \to 0$.

V. CONCLUDING REMARKS

We have shown how the hydrodynamic interaction between a sphere and a plane wall may be introduced into Stokesian dynamics simulations of a suspension of spheres bounded by a single plane wall. The size of the system of equations to be solved is not increased by the introduction of the wall, but the individual resistance coefficients become more complicated to evaluate. This technique can be readily extended to Brownian motion in the presence of a plane and so could be used to simulate the motion of a polymer near a wall, or any problem related to interactions between a plane and Brownian particles. However, the use of images is not attractive when the suspension is bounded by more than one wall, as infinite systems of images are generated. The method adopted by Durlofsky and Brady[8] remains the only one available at present for the numerical simulation of suspensions bounded between *two* walls.

In a future study we shall apply the methods presented here to simulate shear-induced resuspension of sedimenting particles.

ACKNOWLEDGMENTS

This work was supported by Schlumberger Cambridge Research and computer time was provided by the Centre de Calcul Vectoriel pour la Recherche.

APPENDIX: RESISTANCE MATRIX FOR A SPHERE CLOSE TO A PLANE

The self-interaction part of the resistance matrix $\mathsf{I} + (\mathsf{R}_\alpha^{SP})_{FU}$, which gives the force $\mathbf{F}^\alpha$ and couple $\mathbf{T}^\alpha$ on a

single sphere α at a distance $\epsilon a = h - a$ from the plane $z = 0$, can be written as

$$\begin{pmatrix} F_x^\alpha \\ F_y^\alpha \\ F_z^\alpha \\ T_x^\alpha \\ T_y^\alpha \\ T_z^\alpha \end{pmatrix} = \begin{pmatrix} F_x^T & \cdots & \cdots & \cdots & F_x^R & \cdots \\ \cdots & F_x^T & \cdots & F_x^R & \cdots & \cdots \\ \cdots & \cdots & F_z^T & \cdots & \cdots & \cdots \\ \cdots & T_y^T & \cdots & T_y^R & \cdots & \cdots \\ T_y^T & \cdots & \cdots & \cdots & T_y^R & \cdots \\ \cdots & \cdots & \cdots & \cdots & \cdots & T_z^R \end{pmatrix} \begin{pmatrix} U_x^\alpha \\ U_y^\alpha \\ U_z^\alpha \\ \Omega_x^\alpha \\ \Omega_y^\alpha \\ \Omega_z^\alpha \end{pmatrix}.$$

The coefficients F^T, F^R, T^T, and T^R may be obtained from various published sources.[19–25] In the limit $\epsilon \to 0$, the lubrication forms are

$$F_x^T = -\tfrac{8}{5} \ln \epsilon + 0.9588,$$

$$F_z^T = \epsilon^{-1} - \tfrac{1}{5} \ln \epsilon + 0.971\,28,$$

$$T_y^T = F_x^R = -\tfrac{2}{15} \ln \epsilon - 0.2526,$$

$$T_y^R = -\tfrac{2}{5} \ln \epsilon + 6.5089,$$

$$T_z^R = \tfrac{4}{3}\left[\zeta(3) - \tfrac{1}{2}\epsilon \ln \epsilon\right],$$

where $\zeta(3) = 1.202\,05\ldots$.[22] Since T_z^R is not singular in the limit $\epsilon \to 0$, its values were tabulated from the results of Ref. 26.

When a shear flow $u_x = \gamma z$ is imposed, the straining motion E generates a couple $\mathbf{T}^e$ on an isolated particle, and, in the presence of the plane, a force $\mathbf{F}^e$. There are only two nonzero components of the matrix R_{FE}

$$F_x^e = -\gamma Y_{11}^G, \quad T_y^e = -\gamma Y_{11}^H,$$

where the notation Y^G and Y^H is due to Ref. 20. In the limit $\epsilon \to 0$ we have

$$Y_{11}^G = \tfrac{2}{3}\left\{\tfrac{7}{10} \log \epsilon^{-1} - 0.923 + \tfrac{221}{250}\epsilon \log \epsilon^{-1}\right\}$$

$$Y_{11}^H = \tfrac{4}{3}\left\{-\tfrac{1}{10} \log \epsilon^{-1} - 0.0916 + \tfrac{2}{250}\epsilon \log \epsilon^{-1}\right\}.$$

For $\epsilon > 10^{-2}$ we use tabulated values up to a separation $\epsilon = 1$. The first two terms of the multipolar expansion give a good approximation to exact values when $\epsilon > 1$.

[1] A. S. Yoshimura and R. K. Prud'homme, J. Rheol. **32**, 53 (1988).
[2] D. Leighton and A. Acrivos, Chem. Eng. Sci. **41**, 1377 (1986).
[3] T. G. M. Van de Ven, *Colloidal Hydrodynamics* (Academic, London, 1989).
[4] J. F. Brady and G. Bossis, Annu. Rev. Fluid Mech. **20**, 111 (1988).
[5] G. Bossis and J. F. Brady, J. Chem. Phys. **87**, 5437 (1987).
[6] R. J. Phillips, J. F. Brady, and G. Bossis, Phys. Fluids **31**, 3462 (1988).
[7] G. Bossis and J. F. Brady, in *Hydrodynamics of Dispersed Media: 4th EPS Liquid State Conference*, Arcachon, France, May 1988, edited by J. P. Hulin, A. M. Cazabat, E. Guyon, and F. Carmona (North-Holland, Amsterdam, 1990).
[8] L. J. Durlofsky and J. F. Brady, J. Fluid Mech. **200**, 39 (1989).
[9] L. J. Durlofsky, J. F. Brady, and G. Bossis, J. Fluid Mech. **180**, 21 (1987).
[10] J. R. Blake, Proc. Cambridge Philos. Soc. **70**, 303 (1971).
[11] S. Kim and S.-Y. Lu, Int. J. Multiphase Flow **13**, 837 (1987).
[12] A. Meunier, Thèse doctorat, Université de Nice, 1990.
[13] D. J. Jeffrey and J. D. Sherwood, J. Fluid Mech. **96**, 315 (1980).
[14] G. K. Batchelor, J. Fluid Mech. **44**, 419 (1970).
[15] W. B. Russel, E. J. Hinch, L. G. Leal, and G. Tieffenbruck, J. Fluid Mech. **83**, 273 (1977).
[16] H. Brenner, J. Fluid Mech. **12**, 35 (1962).
[17] N. J. De Mestre, J. Fluid Mech. **58**, 641 (1973).
[18] N. J. De Mestre and W. B. Russel, J. Eng. Math. **9**, 81 (1975).
[19] D. J. Jeffrey and Y. Onishi, Q. J. Mech. Appl. Math. **34**, 129 (1981).
[20] R. M. Corless and D. J. Jeffrey, J. Appl. Math. Phys. (ZAMP) **39**, 874 (1988).
[21] D. J. Jeffrey and R. M. Corless, PhysicoChem. Hydrodyn. **10**, 461 (1988).
[22] D. J. Jeffrey and Y. Onishi, J. Appl. Math. Phys. (ZAMP) **35**, 634 (1984).
[23] M. D. A. Cooley and M. E. O'Neill, Mathematika **16**, 37 (1969).
[24] A. J. Goldman, R. G. Cox, and H. Brenner, Chem. Eng. Sci. **22**, 637 (1967).
[25] M. E. O'Neill and K. Stewartson, J. Fluid Mech. **27**, 705 (1967).
[26] G. B. Jeffery, Proc. London Math. Soc. **14**, 327 (1915).